Published in final edited form as:
Biomaterials. 2014 July ; 35(22): 5862–5874. doi:10.1016/j.biomaterials.2014.03.048.

Molecular Factors in Dendritic Cell Responses to Adsorbed Glycoconjugates

Nathan A. Hotaling[1], **Richard D. Cummings**[2], **Daniel M. Ratner**[3], and **Julia E. Babensee**[1]

[1]Wallace H. Coulter Dept. of Biomedical Engineering, Georgia Institute of Technology, Atlanta GA, 30332

[2]Department of Biochemistry, Emory University, Atlanta GA 30322

[3]Dept. of Bioengineering, University of Washington, Seattle WA, 98195

Abstract

Carbohydrates and glycoconjugates have been shown to exert pro-inflammatory effects on the dendritic cell (DC), supporting pathogen-induced innate immunity and antigen processing, as well as immunosuppressive effects in the tolerance to self-proteins. Additionally, the innate inflammatory response to implanted biomaterials has been hypothesized to be mediated by inflammatory cells interacting with adsorbed proteins, many of which are glycosylated. However, the molecular factors relevant for surface displayed glycoconjugate modulation of DC phenotype are unknown. Thus, in this study, a model system was developed to establish the role of glycan composition, density, and carrier cationization state on DC response. Thiol modified glycans were covalently bound to a model protein carrier, maleimide functionalized bovine serum albumin (BSA), and the number of glycans per BSA modulated. Additionally, the carrier isoelectric point was scaled from a pI of ~4.0 to ~10.0 using ethylenediamine (EDA). The DC response to the neoglycoconjugates adsorbed to wells of a 384 well plate was determined via a high throughput assay. The underlying trends in DC phenotype in relation to conjugate properties were elucidated via multivariate general linear models. It was found that glycoconjugates with more than 20 glycans per carrier had the greatest impact on the pro-inflammatory response from DCs, followed by conjugates having an isoelectric point above 9.5. Surfaces displaying terminal α1–2 linked mannose structures were able to increase the inflammatory DC response to a greater extent than did any other terminal glycan structure. The results herein can be applied to inform the design of the next generation of combination products and biomaterials for use in future vaccines and implanted materials.

Introduction

Dendritic cells play a critical role in the adaptive immune response and have been shown to promote tolerance, limit sepsis, and maintain immune cell homeostatsis.[1,2] Dendritic cells

have a variety of pattern recognition receptors (PRRs) that recognize and respond to a plethora of inter- and extra-cellular ligands. C-type lectin receptors (CLRs) are a class of PRRs that are known to bind to carbohydrates. Ligation of CLRs on DCs has shown immense potential for engineering of immune response and controlled immune cell phenotype modulation. Ligation of CLRs has been shown to be key to the regulation of pathogen-induced innate immunity, antigen processing for adaptive immune responses, immune system evasion by pathogens and tumors, and in recognition of self-proteins.[3–7] However, to modulate DC phenotype with CLRs, a more mechanistic understanding of how specific glycan structures and molecular environments affect DC phenotype is needed.

The molecular factors that influence the DC response to surface adsorbed glycoconjugates are unknown. However, charge, via the addition of protamine[8] (small, arginine-rich, nuclear proteins that are highly positive) or poly L-lysine (PLL) has been found to enhance the immunogenicity. Enhanced immunogenicity has been found for a variety of vaccines and therapies including: potent anti-tumor vaccines,[9] non-viral transduction of cells,[10] enhanced siRNA delivery,[11] allergy vaccines[12], etc.[13–15] Furthermore, several cationic glycan carriers have shown increased phagocytosis and DC internalization over that of non-cationic glycoconjugates.[16] Additionally, increased glycan density has been shown to be correlated to increased phagocytosis of glycan coated microparticles.[17–19] Also, Wattendorf et al. [20] found that the efficiency of phagocytosis by DCs increased with increasing amounts of mannose exposed from microspheres' surface.[18] Enchanced phagocytosis with increased glycan density also agreed with findings from other groups who used mannosylated emulsions[17] or liposomes.[19] Sugar structure has also been shown, to cause differential binding specificity for CLRs.[21–26] Several labs have also shown the high specificity of lectins by taking recombinant forms of the receptors and incubating them with glycan structures of interest or with glycan microarrays.[23–25,27–29]

Therefore, the above molecular parameters' (charge, glycan density, and glycan structure) were modulated for glycoconjugate presentation from well surfaces. A high throughput (HTP) assay was then used to assess the effect of the neoglycoconjugates on DC phenotype. A HTP assay was used in lieu of traditional cellular analysis techniques (flow cytometry, mixed lymphocyte reaction, etc.) due to the relatively large amounts of pure glycan needed for such techniques. Complex glycan structures are extremely precious. Thus, the greatest limiting factor to obtaining most immunologically relevant cellular readouts from glycoconjugates other than simple live/dead or adhesion/phagocytosis assays is the availability of these structures in sufficient quantities. New strategies in both synthetic carbohydrate chemistry and biological isolation have improved the speed and quantity of pure glycan able to be obtained; however, these methods still require current cell analysis techniques to be scaled down to volumes typical of high throughput (HTP) assays.[21,30–33]

Materials and Methods

Carrier Functionalization and Purification

Thiol-OEG2 functionalized glycans (Sussex Research) or OEG3-SH (A kind gift from Dr. Daniel Ratner, University of Washington) were reduced in TCEP reducing gel (Pierce) in

sealed spin cups (Pierce) for one hour in degassed buffer 1 (0.1M EDTA, 0.15M NaCl, 0.1M NaH2PO4) at room temperature (RT) while shaking at 600RPM. Glycans were then spun down at 100 RCF and the resultant effluent was immediately added to 1mg/ml Maleimide functionalized BSA (Pierce) in the indicated molar ratio as compared to the maleimide functionalized carrier (0:1, 1:1, 25:1 or 100:1 sugar: carrier ratio). A glycan to protein molar conjugation ratio of 500:1 was used in preliminary studies but no increase in glycan functionalization was seen, thus for these studies, 100:1 was used as the highest molar ratio. Argon gas was passed over the solution and the tubes were sealed with paraffin and allowed to react for 16 hours at RT. After conjugation the glycoconjugates were purified using purification protocol 1:10K Membrane Centrifugal Filter Unit (Millipore) using 9 rounds of 1:10 buffer exchanges against distilled, endotoxin free, water. An identical procedure was followed for the GlcNAc, Man3-Br, Man3-A2, Man4-A2, Man5-Br, and Man5-A conjugates except that only a molar ratio of 100:1 glycan:BSA was used. All glycan thiols were provided by Dr. Daniel Ratner, or produced as discussed below and thiolated via Traut's reagent (Pierce). Conjugates with permanently opened rings were created from these purified glycans via periodate oxidation and sodium borohydride reduction via a standard protocol.[34]

Cationization of Carrier

Three solutions of ethylenediamine (EDA) (0.1, 0.3, or 1.8M) were prepared and pH adjusted to pH 4.5 using 2M NaOH and ultrapure endotoxin free water. Additionally, a 200mg/ml 1-Ethyl-3-[3-dimethylaminopropyl] carbodiimide hydrochloride (EDC or EDAC; Pierce) was prepared using ultrapure endotoxin free water. Using a stock 1mg/ml glycoprotein solution a 1:1 volume ratio of EDA was added to the glycoprotein making the final concentration of EDA 0.05, 0.15, or 0.9M. 0.9M EDA was used in all cases where excess EDA is specified. To these solutions EDC was added to a 7.5mM concentration. The resultant solution was allowed to react for two hours at RT while being shaken at 900RPM. After conjugation the glycoconjugates were purified using purification protocol 1. Figure 1 shows an overview of the process of creating each of the conjugates and gives a list of all 40 conjugates created.

Isolation and Functionalization of Man5-Br

Isolation, functionalization, and quantification of Man5-br was performed via an established method.[21] Briefly, Man5-Br was isolated from ribonuclease B (RNase B) via digestion of RNase B with Pronase. The digested protein then had its N-linked glycans removed by Peptide N-Glycolsidase F (PNGase F). The free reduced glycans were then functionalized with a fluorescent linker, 2-Amino-N-(2-amino-ethyl)-benzamide, (AEAB; A gift from Dr. Richard Cummings, Emory University). The resultant fluorescently modified glycans were then purified via vacuum centrifugation. Finally, the pellet was then dissolved in 1ml of water and glycan fractions were collected using reverse phase HPLC with an excitation of 330 nm and emission at 420 nm.

Preparation and Assessment of ζ-Potential, Mass and Endotoxin Content of Glycoconjugates

Mass spectra of the cationized and non-cationized glycoconjugates were determined using Matrix Assisted Laser Desorption Ionization (MALDI) Mass Spectrometry. The glycoconjugates were first dissolved in ultrapure, endotoxin free water, and then were spotted in a 1:1 vol. ratio with diammonium hydrogen citrate (DHC) onto a MALDI plate. A linear positive detection method was used for the conjugates. Mass profiles were then exported, plotted and the mean of each mass peak was determined.

To determine the isoelectric point, glycoconjugates were diluted to 500ng/ml in ultrapure endotoxin free water and then each conjugate was divided between five different cuvettes. The pH in each cuvette was then adjusted to 3.0, 5.0, 7.0, 9.0, or 11.0 using 1M sterile NaOH or 1M sterile HCl. Using a Malvern Nano-zetasizer (Malvern, Malvern, Worcestershire, UK.) in a cleanroom rated at ISO 6, the ζ-potential and hydrodynamic radius of each solution was then determined. The pH vs the ζ-potential was then plotted and the subsequent isoelectric point of each conjugate was then determined via interpolation of the least squares regression to which point the ζ-potential equaled 0.

The endotoxin contents of the glycoconjugates at a concentration of 100μg/ml (5x the coating concentration used) were measured using an endotoxin assessment kit and the manufacturers recommended protocol (QCL-1000 LAL assay, Lonza). The endotoxin content of all glycoconjugates was determined to be less than 0.2 EU/mL (data not shown). The FDA limit for endotoxin content is 0.5 EU/mL and thus all conjugates had less than half the safe amount of endotoxin. Furthermore, all mannose conjugates were below the detection limit of the assay for endotoxin content. All conjugates tested in this paper were from a single preparation.

Enzyme Linked Lectin Assay for Adsorbed Glycoconjugates

A 96-well tissue culture polystyrene (TCPS, NUNC) plate was coated with 20μg/ml of the each glycoconjugate overnight at RT. Next, the plates were washed and blocked for two hours at 37°C with 5mg/ml biotin free HSA in 0.1M NaHCO3 and 0.1% TWEEN 20. After blocking the plates were washed 5x with wash solution 1 (1x PBS, 0.01% TWEEN 20, 0.5mg/ml biotin free HSA). Next, a lectin specific for the given sugar 15 μg/ml Narcissus pseudonarcissus-biotin (NPA-biotin) (EY Labs; specific for α-D-mannose) or 15 μg/ml Concanavalin A-biotin (ConA-biotin) (Sigma; specific for mannose or glucose) was incubated with the adsorbed conjugates for two hours at 37°C. The plates were then washed 5 times with the wash solution 1 and 50μl of a streptavidin-HRP (BD Pharmingen) solution diluted 100x with PBS from stock was added to each well and allowed to incubate in the well for 2hrs at RT. The plate was then washed 5x more times with wash solution 1 and a TMB (3,3′,5,5′-tetramethylbenzidineperoxide) substrate (BD Pharminogen) was added and the plates allowed to develop for 10 minutes. Then, a 1:1 volume ratio of 1.0N sulfuric acid was added to stop the reaction and the absorbance at 450nm was determined, using Tecan Infinite F500 microplate reader (Tecan Männedorf, Switzerland).

Dendritic Cell Culture

Dendritic cells were isolated via a standard protocol.[35] Briefly, human blood was collected from healthy donors with informed consent and heparinized (333 U/ml blood) (Abraxis Pharmaceutical Products, Schaumburg, IL), in accordance with protocol H10011 of the Institutional Review Board at Georgia Institute of Technology. Dendritic cells were derived from human peripheral blood mononuclear cells (PBMCs). PBMCs were isolated by differential centrifugation using lymphocyte separation medium (Cellgro MediaTech, Herndon, VA). After the lysis of residual erythrocytes with RBC lysis buffer (155 mM NH4Cl, 10 mM KHCO3, 0.1 mM EDTA), the PBMCs were washed with D-PBS and then PBMCs were plated at a concentration of 5x106 cells/ml in DC media [RPMI-640 (Invitrogen), 10% heat inactivated FBS (Cellgro MediaTech) and 100 U/ml of penicillin/ streptomycin (Cellgro MediaTech). After 2 hours of incubation for the selection of adherent monocytes, the dishes were washed and the remaining adherent monocytes were incubated with DC media, supplemented with 1000 U/ml GM-CSF and 800 U/ml IL-4 (PeproTech, Rocky Hill, NJ), for 5 days to induce the differentiation of monocytes into immature DCs (iDCs).

Exposure of DCs to glycoconjugate adsorbed wells

On day 4 of DC derivation 20μg/ml glycoconjugate solutions were added to wells of a 384-well tissue culture polystyrene (TCPS) plate in quadruplicate. The solutions were allowed to incubate in the wells overnight at RT. Next, all the wells were washed with complete DC medium and blocked for two hours at 37°C with 5mg/ml biotin free HSA in 0.1M N aHCO3. After blocking the plates were then washed 5x with complete DC media.

On day 5 after isolation, loosely adherent and non-adherent cells containing iDCs were harvested and resuspended in DC media. These cells were then plated in 40 μl of cell suspension (3.0x104 DCs) on glycoconjugate adsorbed wells in quadruplicate. The extent of DC maturation was compared to untreated DCs (iDCs) for the negative reference control and lipopolysaccharide (LPS) (1 mg/ml; E. coli 055:B5; Sigma)-treated DCs (mDCs), adsorbed zymosan A (Saccharomyces cerevisiae; Sigma), or Mannan (Saccharomyces cerevisiae; Sigma) for the positive reference control for the inflammatory maturation factor (IMF, mDCs). The positive control for the tolerogenic maturation factor (TMF, tDC) is human IL10 and human IFNα (R & D Systems) treatment of DCs for 24 hours at 3500 units/ml and 35000 units/ml respectively.

High Throughput Evaluation of Dendritic Cell Phenotype to Adsorbed Glycoconjugates

Differentially-treated and reference control DCs were harvested after 24 h for analysis using an HTP method previously described with modifications. [36] Briefly, DCs were placed in treatment wells on day 5 after isolation at 7.5x105 cells/ml. After 24 hours all treated DCs and controls were transferred via multi-channel pipette to a black 384-well filter plate (Pall Life Sciences), and the supernatants were immediately collected into a 384-well plate through the filters by stacking the filter plate on top of the 384-well collection plate and centrifuging at 300 RCF for 4 min. While spinning down the filter plate, wells of the TCPS plate with glycoconjugates adsorbed to them were incubated with Non-Enzymatic Cell Disassociation Solution (CDS; Sigma). The CDS treated cells were then lightly pipetted up

and down and transferred to the black filter plate after its first spin-down. The CDS was removed by stacking the filter plate on top of a new collection plate and centrifuging at 400 RCF for 4 min. To the retained cells 50 μl of 0.05% formaldehyde solution was added and the cells were allowed to fix for 40 minutes at room temperature while being shaken at 600 RPM. The formaldehyde solution was then removed via centrifugation at 400 RCF for 4 minutes. The cells retained in the wells were assessed for phenotype by immunostaining using antibodies anti-CD86-PE (Clone BU63; Ancell), anti-DC-SIGN-FITC (Clone 120507; R & D Systems), and anti-ILT3-AF647 (Clone ZM4.1, Biolegend). IgG1-PE (clone MOPC31C; Ancell) and IgG2B-FITC (clone 133303; R&D Systems) isotype-stained DCs were measured for background fluorescence subtraction. CD86 is a costimulatory molecule that is up-regulated upon pro-inflammatory DC maturation,[36] Dendritic Cell-Specific Intercellular adhesion molecule-3-Grabbing Non-integrin (DC-SIGN) is an endocytic receptor that is slightly down-regulated upon pro-inflammatory maturation,[36] and Immunoglobulin-like transcript 3 (ILT3) is a member of the immunoglobulin superfamily which signals via the immunoreceptor tyrosine-based inhibitory motifs and is up-regulated upon anti-inflammatory DC maturation.[37] After 30 minutes of staining the cells were washed three times with a wash solution of 0.1% BSA and 2mM EDTA in PBS, pH 7.20. The excitation/emission wavelengths for each fluorophore are 535/590 for PE, 485/535 for FITC, and 650/668 for AF647. The geometric mean fluorescent intensities (gMFIs) were then determined using the appropriate wavelengths for excitation and emission using a Tecan Infinite F500 microplate reader, and the ratio of respective gMFIs were determined as CD86/DC-SIGN, a cell number independent metric named “inflammatory maturation factor” (IMF), and ILT3/CD86, a cell number independent metric named “tolerogenic maturation factor” (TMF) to represent DC phenotypic outcomes. Figure S 1 in the supplemental shows a schematic of the 384 well plate high-throughput methodology for assessment of DC phenotype to adsorbed glycoconjugates.

For the studies where EDTA was used to block CLR receptors, cells were treated with either 10mM or 5mM EDTA for one hour at 37°C before exposure to 1 μm bead adsorbed glycoconjugates. Cells were then transferred, with media still containing EDTA, to the wells with the glycoconjugate coated beads and the subsequent phagocytosis of the 1 μm beads was assessed after 4hrs or DC phenotype assessed via the above HTP methodology after 24hrs. For assessment of phagocytosis, cells were transferred to a filter plate, washed with PBS, fixed with 1% formaldehyde for 30 minutes, washed again with PBS, and incubated with 0.1% trypsin for 1 minute. Cells were then washed three times with PBS, and visualized via a Nikon Ti fluorescent microscope (Nikon, Tokyo).

Cell Viability and Cytotoxicity of Glycoconjugates

Cytotoxicity associated with adsorbed glycoconjugate treatment was assessed via live/dead staining of the cells using standard methodology.[38] Briefly, cells were treated with adsorbed glycoconjugates as in the HTP methodology for 24 hours. Cells were transferred to a 384 well filter plate and supernatants removed as in the HTP methodology. The cells were then stained with calcein AM and ethidium homodimer-1 for 40 minutes. Cells were then washed 3x with PBS and the fluorescent intensity of the cells (excitation/emission 495/530 nm – live and 528/630nm – dead) was determined using the Tecan Infinite F500 microplate

reader. Additionally, the amount of cell apoptosis was of interest due to possibility that cells were impermeable to Ethidium homodimer but still in the process of apoptosis. To assess apoptosis DCs were stained for Annexin V-FITC and the extent of binding to phosphatidylserine was measured via the HTP format. No treatments showed a significantly different viability from untreated cells and no treatment showed a statistical change in Annexin V binding (data not shown).

Statistical Analysis

To observe significant differences between all sample groups in pairs, a pairwise two-way ANOVA followed by Tukey's posttest was performed using SAS software (Cary, NC), and the p-value equal to or less than 0.05 was considered significant. Significance of general linear statistical model parameters discussed in section 4.2.12 and seen in Equation 1a, Equation 1b and Equation 2 was determined by T value in reference to referent group discussed in the Statistical Modeling section below.

Statistical Modeling

An in-depth discussion of the statistical models and data used can be found in the supplemental materials section. Briefly, general linear models were constructed and IMF or TMF were modeled as functions of conjugate isoelectric point, ligand attached, density of ligand, and donor. An in-depth analysis of these variables can be seen in Tables S1A–C and Tables S2A–B in the supplemental materials section. To determine the level at which isoelectric point and density became statistically significant both isoelectric point and density were modeled as categorical variables. The hypotheses tested in these models was that when controlling for all other measured factors the level of cationization or ligand density would significantly influence IMF/TMF. The variable *donor* was included in the analysis to account for the repeated measures of each donor across conjugates and to help limit the large inter-donor variability that is seen with primary donors. The reference donor was chosen at random and because all other factors control for donor in their calculation of beta, no influence on the calculated coefficients or their significance was seen when changing between reference donors. Equation 1a (IMF) and Equation 1b (TMF) are shown below.

$$\mathrm{IMF}=\beta_1+\beta_2{}^{*}Isoelectric\_\ cat+\beta_3{}^{*}ligand+\beta_4{}^{*}density\_\ cat+\beta_5{}^{*}donor \quad \text{Equation 1a}$$

$$\mathrm{TMF}=\beta_1+\beta_2{}^{*}Isoelectric\_\ cat+\beta_3{}^{*}ligand+\beta_4{}^{*}density\_\ cat+\beta_5{}^{*}donor \quad \text{Equation 1b}$$

The reference for the model shown in Equation 1a and b was any donor who was treated with an adsorbed conjugate that had no cationization, no ligand immobilized and thus no density of ligand. Also, it was found that low density conjugates were linearly related to the conjugates with no ligand and thus these conjugates were excluded from the model.

Another set of general linear models were constructed to analyze the effects of various glycan structures on IMF and TMF. In these models optimized conjugates from the previous model were used and IMF and TMF were modeled as a function of glycan structure, ligand

density, and donor. The hypothesis tested in these models was that glycan structure would significantly affect IMF or TMF. Level of cationization was not modeled in these equations because all conjugates had approximately equal isoelectric points and thus this was an uninformative variable. Upon modeling it was found that TMF was not significantly influenced by any glycan structure and thus no model is shown herein for TMF. However, IMF was significantly affected by glycan structure and thus its model can be seen in Equation 2. The seven structural motifs assessed in Equation 2 were *None, OEG, N-acetylglucosamine (GlcNAc), Mannose (Man), Glucose (Glc), Terminal Branched Mannose (Branch)*, and *α1–2 Terminal Mannose (Alpha)*. Which structures were included in these groupings can be seen in Table S2B.

The donor variable was included to account for the repeated measures of each donor across conjugates and to help limit the large inter-donor variability that was seen with primary donors. Isoelectric point was not included in this model because all conjugates were highly cationized and thus their isoelectric points only varied between 9.9 and 10.1. It was also found that OEG conjugates were linearly related to the conjugates with no ligand and thus these conjugates were excluded from the model.

The reference donor was chosen at random and because all other factors control for donor in their calculation of beta, no influence on the calculated coefficients or their significance was seen when changing between reference donors. For Equation 1a, Equation 1b, or Equation 2 the R^2 and correlation coefficients between variables were compared to determine how well the model fits the data. Furthermore, the IMF data has historically been shown to be approximately normal and the variance of the data remains constant across all samples thus the linear model used herein is further deemed as a valid analysis method.[36]

$$\mathrm{IMF}=\beta_1+\beta_2{}^{*}structure+\beta_3{}^{*}density\_\ cat+\beta_4{}^{*}donor \quad \text{Equation 2}$$

Results

Charge and Density of Glycoconjugates

Increasing the molar ratio of thiolated glycan to BSA resulted in increased glycan density on glycoconjugates as determined using MALDI mass spectrometry (Figure 2A). Specifically, mean functionalization levels, presented as average number of glycans/BSA molecule were 26, 9.6 and 2 for molar ratios of glycan to BSA of 100:1, 25:1 and 1:1, respectively. These levels of glycan functionalization were not affected by type of glycan presented (mannose or glucose) or the level of catioziation with EDA concentration, as shown in Figure 2A. Control non-glycan modified BSA conjugates, presenting solely the OEG linker, when reacted at the same molar ratios used for glycan presentation, had no detectable increase in mass.

Figure 2B shows that reacting glycoconjugates with higher molarities of EDA resulted in increased glycoconjugate isoelectric point. Mean cationization levels, as assessed by isoelectric point determination from conjugate ζ-potential, were 4.7, 8.3, 9.0, and 10 for 0.0, 00.05, 0.15, and 0.9 molar concentrations of EDA respectively. Glycoconjugate charge was

nominally affected by type of ligand presented (OEG, mannose or glucose) or the number of ligands immobilized per conjugate, as shown in Figure 2B. Also of interest was that each increase in molarity of EDA caused an ~ 1 unit increase in pI of the glycoconjugate.

Enzyme Linked Lectin Assays of Glycoconjugates

The characterized glycoconjugates from Figure 2 were adsorbed to the wells of a 96 well TCPS plate and functional binding of lectins to glycan moieties was assessed via ELLA. Figure 3 shows that the adsorbed conjugates were able to present glycans in a biologically available display by showing that plant lectin, ConA (Figure 3A–C) and NPA (Figure 3D), binding increased with increased glycan density on adsorbed glycoconjugates. Additionally, Figure 3D shows that the presentation of glycan from the adsorbed glycoconjugates was structure-specific as NPA, a mannose specific lectin, bound mannose conjugates and not glucose. Figure 3A–C also showed that as cationization level of conjugate increased so did non-specific lectin binding. Finally, the signal from the non-cationized, low, and medium cationized glucose conjugates (Figure 3A,C) is significantly lower than that of the same conjugates when conjugated to mannose (Figure 3B). However, the trend between these conjugates is similar as can be seen from the subset of Figure 3A shown in Figure 3C.

Dendritic Cell Phenotype in Response to Adsorbed Glycoconjugates

Using the HTP method, DC phenotype was found to be significantly altered by adsorbed, high density, cationized mannose glycoconjugates. Figure 4A shows that any level of cationized, high density, mannose glycoconjugate (L-, M-, or H-BSA-Man 100) significantly increased the pro-inflammatory DC maturation factor, IMF, and that no other adsorbed glycoconjugate statistically affected DC phenotype. Figure 4B shows no adsorbed glycoconjugate increased the tolerogenic reporter, TMF, as compared to untreated cells. In Figure 4A positive controls mDC (LPS treated DCs), adsorbed mannan, and adsorbed β-glucan all showed a statistical increase in DC levels of IMF as compared to untreated cells (iDC). When comparing the general trends in IMF and TMF to glycoconjugate charge and density in Figure 4A and Figure 4B an inverse trend of material properties to IMF and TMF appeared to be present. The apparent shift in trends was analyzed with the statistical model found in Equation 1B and is discussed in more detail below.

Figure 4A also shows that the level of DC IMF for the cationized glucose conjugates was raised as was the DC IMF for the mannose conjugates and it was desired to show that this activation was not due to non-specific glycan activation of DCs. Thus, the highly cationized mannose and glucose glycoconjugates' glycans were permanently reduced to their open ring conformation so that the conjugates were chemically identical but were unable to be bound by lectins. DC phenotype was then assessed to the reduced, adsorbed, conjugates via an identical method as above and no statistical increase in DC levels of IMF or TMF was seen from the reduced conjugates, as seen in Figure S2.

Modeling of the DC Response to Adsorbed Glycoconjugates

General linear models were created to determine which molecular factors significantly affected DC levels of IMF (Equation 1a) or TMF (Equation 1b). Results from Equation 1a (Table 1) show both glycan density and charge to be significant predictors of IMF; with high

glycan density having the greatest positive impact on DC levels of IMF ($\beta = 0.38$). Conjugates with a high cationization level had the next largest impact on DC levels of IMF ($\beta = 0.17$). The variables medium isoelectric point, medium density also significantly increased DC levels of IMF. Of note is that low isoelectric point, pI< 7.5, and any ligand had no significant impact on DC levels of IMF when controlling for all other factors measured.

Equation 1b showed isoelectric point, density of conjugates, and donor all significantly changed DC levels of TMF. Results from this model, seen in Table 2, show that the highest density and highest cationization levels caused significant decreases in DC levels of TMF and that conjugates with an isoelectric point less than 7.5 showed a significant positive increase in DC levels of TMF. Interestingly, when comparing significance of IMF factors to those of TMF the inverse trend indicated in Figure 4 was shown to be valid.

The R2 of the models seen in Equation 1a and b was calculated to determine the goodness of fit and the appropriateness of these models in assessing the data. Equation 1a and Equation 1b had an adjusted R2 of 0.639 and 0.539, respectively. This indicates that approximately 64% (Equation 1a) and 54% (Equation 1b) of the variance seen in the data can be explained by the model used. These R2 values were considered fairly good for the relatively small sample size used (13 donors) and high variability of primary donors.

Inhibition of DC Internalization of Glycoconjugates

The contribution of calcium (implicating lectin interaction) in mediating the interaction of DCs with the glycoconjugates was assessed as shown in Figure 5A–D which shows micrographs of DCs incubated with H-BSA or with H-BSA-Man100 coated fluorescent beads in the presence of EDTA (Figure 5B and D, respectively) or without (Figure 5A and C, respectively). Figure 5A and C show that, without EDTA, DCs internalized many beads (frequently >10 beads per cell) regardless of type of ligand presented. However, phagocytosis of beads in the presence of EDTA was attenuated as shown in Figure 5B and D for H-BSA and with H-BSA-Man100 coated fluorescent beads, respectively. DC internalization of beads was analyzed via manual counting of beads per cell and averaging over multiple fields of view. However, for bead treatments where EDTA was not administered bead internalization per cell was too high to obtain accurate bead counts. For treatments where 5mM EDTA was added bead internalization of cells averaged to be slightly less than 1 bead per cell for both HBSA and HBSA-Man 100 conjugates.

Assessment of DC phenotype to adsorbed HBSA-Mann 100 conjugates in the presence and absence of EDTA was performed and can be seen in Figure 5D. Only DCs treated with adsorbed H-BSA-Man100 conjugates without EDTA treatment had a statistically significant up-regulation of IMF as compared to the value for iDCs.

Dendritic Cell Phentotype in Response to Diverse Sugar Structures

The lack of significance of ligands, comparing between glucose and mannose, in Equations 1a and b was surprising given the known specificity of lectins for different glycan structures. Given that DCs were responsive to presented mannose, DC response to adsorbed HBSA conjugates with six different mannose structures (Figure 6A) was assessed via the HTP methodology. Figure 6B shows that both H-BSA-Man and H-BSA-Man5-A2 increased

levels of DC IMF to a statically significant extent. Interestingly, an α1–3, α1–6 branched structural homolog for Man5-A2, Man5-Br, showed no effect on DC levels of IMF. Furthermore, an α1–3, α1–6 branched trimannose (Man3-Br) also showed no effect on DC levels of IMF. An additional control sugar (N-acetyl glucosamine) was added for these experiments to further validate that any non-specific glycan presentation from the adsorbed highly cationized BSA would not affect DC levels of IMF. Figure 6B also shows that the positive control, mDC, and the highly cationized BSA-Man conjugate showed a statistical increase in IMF as compared to the level for iDC. Additionally, H-BSA-GlcNAc, and controls H-BSA and H-BSA-OEG showed no increase in DC levels of IMF as compared to that of control iDCs.

Figure 6 showed that two different mannose structures were able to significantly increase DC levels of IMF. Thus, a model that grouped glycan structures based on terminal glycan motif was made, using Equation 2, to predict the structural relevance of glycans on DC expression levels of IMF, indicating maturation. In this model structural variables glucose, mannose, and alpha all statistically increased DC levels of IMF as shown in Table 3. No density variable had a statistically significant influence on DC phenotype nor did any α1-3, α1-6 branched mannose structure or N-acetylglucosamine. Of note is that low and medium density levels of ligand presentation reduced IMF and all ligand classes analyzed increased DC IMF. Because the results from Figure 4 clearly show that no mannose or glucose conjugate had a significant effect on DC levels of TMF, only IMF results were assessed. The R2 of the model shown in Equation 2 was calculated to determine the goodness of fit and the appropriateness of these models in assessing the data and was found to have an adjusted R2 of 0.622.

Discussion

Figure 4A shows that only the highest density (>20glycan/protein) cationized mannose conjugates significantly increased the DC IMF levels. The increased inflammatory response is supported by literature which has shown the importance of cationization[9] and high glycan density[39] to lectin binding. Figure 4 also shows that uncharged glycoconjugates did not change DC IMF levels over untreated DCs. Further, when the DC response to charged and uncharged glycoconjugates was compared a differential DC phenotype was seen; indicating that BSA does not provide a specific molecular niche that enables glycan recognition. Models in Equation 1A and B further support these results by showing that both isoelectric point and glycan density significantly increase DC IMF levels. When the β coefficients in Equation 1A were compared both high density and high cationization had the largest effect on IMF. Additionally, “high” glycan density had twice the magnitude of impact of “high” isoelectric value on DC IMF. The magnitude of the beta coefficients indicate that density is the most important factor for consideration when designing glycoconjugates to increase the pro-inflammatory DC phenotype. Interestingly, the models in Equation 1a and Equation 1b both indicate that ligand was not a significant factor in either IMF or TMF. The lack of significance of ligand was surprising given that in the ANOVA analysis only mannose conjugates showed a significant increase in IMF over untreated cells. In the models found in Equation 1A and B all levels of cationization and density for each ligand were pooled together for comparisons. Thus, if interaction between

glycan and charge or density was necessary for activation this interaction would be lost in the models in Equation 1A and B. Thus, two-way interaction variables between ligand, cationization level, and density were introduced to the model (equation not shown) to overcome ligand pooling limitations. However, due to the limited number of donors tested in the model, these interaction variables caused the model to not converge and thus could not be used. Due to this limitation a further glycan structure assessment was performed in Figure 6 to ensure that the assay could differentiate between glycan structures when displayed from well surfaces and is discussed in more detail below.

An inverse correlation between the beta coefficients found in Equation 1A and beta coefficients found in Equation 1B was also found when comparing the results of the models. Inverse beta coefficient signs indicate an inverse DC phenotype correlation derived from material properties in response to glycan moieties. Inverse correlation between presented glycan characteristics inducing pro-inflammatory or anti-inflammatory DC responses would intuitively be expected as they are measuring opposite regions on the DC phenotypic spectrum. Also, the beta coefficients for all variables in the TMF model were lower in magnitude from those of the IMF model. The lower magnitude indicates that the variables assessed play a smaller roll in modification of DC TMF than they do in the IMF. Further, the low magnitude of the beta coefficients indicates that the most important factors for modification of DC TMF might not have been assessed in the studies herein. Thus, future studies should focus on new variables, such as different glycans and linkers, for a more thorough understanding of how to optimally modify DCs toward a tolerogenic phenotypic state.

Mannosides were chosen for the study in Figure 6 because they are the most extensively studied and understood of all ligands for CLRs on DCs with known phenotypic effects.[23,40–43] Other work has previously shown that man, triman (α1-3 α1-6), or mannan immobilized on phagocytosable beads had different extents of DC uptake.[20] In this study it was found that the mannan coated particles had the highest uptake, followed by the single mannose, with the lowest phagocytosis seen in the triman functionalized particles; which agrees well with the activation shown in Figure 6 and the results found from Equation 2.

One of the glycan structures used had a base GlcNAcβ1-β4GlcNAc motif that was modified with AEAB and a thiol. This structure is distinct from the other glycans which are homogenous for mannose and have no fluorescent linker (AEAB) attached to them. This seemingly random sugar was chosen because this glycan structure is a common motif found in humans to which many other glycan motifs are added.[44] The other glycan structures tested are not commonly found in healthy humans and are instead found on Entamoeba and in some forms of lymphoma.[45,46,47] The change in linking chemistry was chosen because the sugar was isolated from a protein, RNase B, and not made via synthetic carbohydrate chemistry and thus had to be identified in HPLC for purification and isolation. Carbohydrates modified in this way have been used frequently in glycan arrays made by the Consortium for Functional Glycomics, one of the largest providers of carbohydrate resources to the glycan community, and thus it is seen as unlikely to of caused the difference in cell response between it and its structural homolog Man-5-A2. In support of this conclusion, Feinberg et. al.[29] found that any glycan structure with a terminal α1-α2 man-

man linkage showed a higher binding affinity for DC-SIGN than did those structures that did not. Also, Wattendorf et al.[20] showed that for Man3-Br conjugates presented from a non-fouling PEG backbone produced no change in CD80, CD86, and MHCII from iDCs which also agrees with the results herein.

However, an unbiased analysis of glycan structure motifs and DC activation was desired to determine if the response that was uncovered in this report truly correlated with that found in the literature. Thus, the model seen in Equation 2 was created. The glycan grouping found in Equation 2 was selected by running models with all combinations of glycan motifs. Grouping glycans via terminal linkage of glycan, via α1-3, α1-6 branched or α1-2 mannose, showed the highest statistical significance for ligands and also produced the greatest R2 value for the model. Furthermore, the resultant glycan groups used in Equation 2 yielded the most significant grouping of structures. Algorithmically generated grouping was seen as a strength of the model as the data was used to determine the underlying trends and no bias was introduced by the researchers.

The α1-2 terminal linked mannose structures have been shown to be expressed on the surface of Entamoeba[45] and in class E Thy-1 negative mutant lymphomas. [46,47] The Thy-1 negative mutants show an inability to produce dolichol-P-mannose and thus cannot effectively modify the block transferred N-glycan core structure.[47,48] Thus, it is hypothesized that since these structures are never found in healthy tissue and only in a pathogen, Entamoeba, or on lymphomas, that CLRs have evolved to recognize these structures as danger or pathogen associated molecular patterns (DAMPs or PAMPs) and become activated by them. Furthermore, that CLRs could recognize these structures was not surprising considering the affinity studies that were completed by Feinberg et. al., Ratner et. al. and the Consortium for Functional Glycomics open database.[23,29,49] A complex lectin specificity for glycans is consistently shown in these studies and high structural specificity is common among lectins. For example, the Consortium has shown that DC-SIGN is able to distinguish between two isoforms of Man3, one branched α1-3, α1-6, the other linear α1-3, α1-2, with high prejudice since version 2.1 of its Mammalian Printed Array.

The significance of the structural factors and of density indicates a trend that could be used in future studies that attempt to model DC interaction with complex carbohydrate structures. Combining inferences made from the models in both Equation 1a, Equation 1b and Equation 2 it could be theorized that permutating a limited number of terminal glycan structural motifs across densities could account for the largest impact on DC phenotype. However, this conclusion is seemingly confounded in Table 3 because in this model density is not a significant factor. However, all conjugates in Table 3 were conjugated at the 100:1 molar ratio. Thus, the variance in number of ligands per BSA was much smaller than that found in the models shown in Equation 1A and B. The lack of variance led to density being a relatively uninformative variable in this model. However, it was retained in the model so that future researchers are able to compare their glycoconjugates to those tested here regardless of density or formulation used.

To help ensure that activation of DCs was occurring through CLRs, DCs were incubated with the adsorbed high density mannose and glucose conjugates in the presence and absence

of EDTA. Concentrations of EDTA were chosen based on previous literature values and because they were known to inhibit CLR binding in DCs without activating DCs.[35,50] All CLRs are calcium-dependent and thus incubating cells with a calcium chelater, EDTA, has been shown to impair the function and signaling of a variety of CLRs.[44] A pan CLR inhibitor rather than a specific antibody was chosen as an inhibitor because of the numerous receptors capable of binding mannose conjugates on DCs.[51] Additionally, several of these receptors have no known blocking antibody and others have not had the molecular signaling pathway through which they signal defined[51] Thus, treating DCs with EDTA was seen as the best approach for confirmation of CLR interaction with the conjugates. Blocking antibodies for the best characterized CLRs that bind mannose (DC-SIGN and MMR) were tried but no significant decrease in bead phagocytosis was found which agrees with several reports in the literature that show redundant function of CLRs.[52,53]

The HTP assay used herein was derived from an assay developed by Kou et. al.[36] This assay has shown an excellent correlation between the IMF reporter and a total pro-inflammatory DC phenotype as validated by multiplex cytokine analysis and extensive flow cytometry. [36,54,55] Thus, using this assay as a screening technique for large glycan arrays was seen as an excellent proxy for in-depth cellular analysis, which wasn't possible due to limited quantities of pure glycan structures. Using the HTP assay and a common non-immunogenic[19,58–62] protein carrier for glycans, BSA [56,57], the DC response to engineered surface adsorbed glycoconjugates was able to be assessed in a manner that has never been possible before in glycobiology.

Mass spectra of the conjugates showed that glycan moieties scaled in density with increased molar ratios of glycan. The scaling agrees well with results shown by Oyelaran et al.[39] However, it was found that OEG conjugates did not appear to scale with increased molar ratios. The OEG conjugates were created at the same time with identical conditions to those of the other glycoconjugates. It was therefore concluded that the OEG linker mass was small enough that the number of functionalizations per BSA were within the experimental error of the MALDI mass spectra. While no direct evidence of this has been shown in the literature, the average standard deviation of the mass profile for each of the OEG100 conjugates was 11774 ± 6180 Da. With an average standard deviation of over 6kD and a maximum weight of OEG ligands reaching approximately 3kDa it would be no surprise that the OEG linker weight could be lost in the noise of the mass profile. Figure S3 in the supplemental shows two typical sets of MALDI mass profiles for the OEG conjugates.

Figure 3A–C showed a non-specific increase in lectin binding with increased cationization of adsorbed glycoconjugate. This was unexpected but the natural isoelectric point of ConA is approximately 5.0 and thus its negative zeta potential at neutral pH could lead it to non-specifically bind more strongly to the cationized conjugates. Enhanced association with the adsorbed protein would allow for longer and more intimate association of the lectins with the presented glycans. Longer and stronger lectin association has been hypothesized to lead to more multivalent interaction with the lectins and thus higher overall binding of the lectins to the cationized conjugates.[63]

This study assessed the DC response to a diverse array of synthetic glycoproteins with the goal of obtaining a more fundamental understanding of DC response to glycoconjugates. However, these conjugates were not explicitly defined as there was inherent variability in their formulation, adsorption, and charge. Even within a single batch of glycoproteins MALDI showed a range of sugar modifications to protein carriers. This heterogeneity leads to higher variability in results and difficulty in recapitulation of interesting findings because formulations cannot be exactly repeated even under identical reaction conditions. Furthermore, direct comparisons between one conjugate or formulation to another are not strictly possible due to this variability. Thus, modeling the data allowed for decoupling of this variability and assured that the data and inferences elucidated from these studies could be applied to other similar systems. Additionally, modeling has the advantage of being able to control for factors such as density when comparing charge states even if the conjugates did not have identical densities. This allowed for assessment of magnitude of importance of a factor or association between variables which is valuable when trying to identify optimum combinations of factors for the design of future biomaterials. Most importantly, the results from this modeling can be used to predict the most influential factors for design of adsorbed glycoconjugates for response from DCs. Molecular factors of glycan presentation to DCs was modeled in such a way as to remove batch or sample variability from the underlying factors of importance which is important for future studies comparing results to these models.

While this study uncovers a mechanism for alteration of DC phenotype with adsorbed glycoconjugates an understanding of the underlying mechanism for why this is occurring was not explored. The study completed here indicates that for adsorbed glycoconjugates highly cationized, high density mannose conjugates are able to induce a pro-inflammatory phenotype in DCs. However, why this is occurring, what specific receptors are being used, and what downstream cytokine and chemokine effectors are being produced after interaction with these adsorbed glycoconjugates needs to be elucidated. An understanding of the signaling pathways, molecular intermediaries, and downstream effectors would allow for a greater mechanistic understanding of what was uncovered in this report. This work is ongoing and the results from these studies will provide more opportunities for engineered ligands to influence DC phenotype.

Conclusions

Using multivariate statistical modeling, a method for the alteration of DC phenotype with adsorbed glycoconjugates was identified—providing fundamental insights into the DC interaction with surface presented glycoconjugates. This study successfully quantified the relative effect of density and cationization of adsorbed glycoconjugates on the pro-inflammatory DC response, and demonstrated that factors for promotion of IMF were inversely correlated to factors that promoted TMF. This represents the a statistical validation of this effect. The DC pro-inflammatory response to oligomannose structures presented from adsorbed conjugates was established to be enhanced for Man5-A2 but not its structural homolog Man5-Br. When these structures were grouped in a model by terminal glycan motif it was found that terminal structural motifs played a significant role in the prediction of DC IMF. This study also determined that terminal glycan structural motifs have been found to

correlate to DC phenotype in response to adsorbed glycoconjugates across a variety of glycan structures. Finally, this study established that general linear modeling of DC interaction with adsorbed glycoconjugates produced highly predictive models, $R2 \geq 0.59$ for all models, for a study using primary human donors with relatively small sample sizes ($N<20$). This report provides a framework for the analysis of data related to the differential biological response to glycosylated species. The results show the potential of multivariate linear modeling in determining the relative significance of other molecular factors (linker charge, length, and flexibility, polymeric carriers, etc.) that could be relevant to phenotype modulation of DCs via CLRs. These results serve as the first step toward harnessing glycans and glycoconjugates for non-phagocytosable immunomodulatory biomaterials.

Supplementary Material

Refer to Web version on PubMed Central for supplementary material.

Acknowledgments

We would like to acknowledge Dr. Xuezheng Song from Emory University for his invaluable expertise with glycan isolation and functionalization. Also we would like to thank David Smith for the generous contribution of AEAB, mass spectrometer, and lab space. We also wish to acknowledge the Consortium for Functional Glycomics and NIH Grants GM62116 and GM098791 for contributing glycans and other resources. We would like to acknowledge support through the NIH Cell and Tissue Engineering Doctoral Training Grant and through the National Center for Advancing Translational Sciences of the National Institutes of Health under Award Number UL1TR000454, research supported by NIH 1RO1EB004633-01A1, 1R21EB012339-01A1.

References

1. Steinman RM, Hawiger D, Nussenzweig MC. Tolerogenic dendritic cells. Annu Rev Immunol. 2003; 21:685–711. [PubMed: 12615891]
2. Steinman RM, Banchereau J. Taking dendritic cells into medicine. Nature. 2007; 449(7161):419–26. [PubMed: 17898760]
3. Van Die I, Cummings RD. Glycan gimmickry by parasitic helminths: a strategy for modulating the host immune response? Glycobiology. 2010; 20(1):2–12. [PubMed: 19748975]
4. Unger WW, van Kooyk Y. “Dressed for success” C-type lectin receptors for the delivery of glyco-vaccines to dendritic cells. Curr Opin Immunol. 2011; 23(1):131–7. [PubMed: 21169001]
5. Aarnoudse CA, Vallejo JJG, Saeland E, van Kooyk Y. Recognition of tumor glycans by antigen-presenting cells. Curr Opin Immunol. 2006; 18(1):105–11. [PubMed: 16303292]
6. Geijtenbeek TBH, van Vliet SJ, Engering A, ’t Hart BA, van Kooyk Y. Self- and nonself-recognition by C-type lectins on dendritic cells. Annu Rev Immunol. 2004; 22:33–54. [PubMed: 15032573]
7. Mascanfroni ID, Cerliani JP, Dergan-Dylon S, Croci DO, Ilarregui JM, Rabinovich GA. Endogenous lectins shape the function of dendritic cells and tailor adaptive immunity: Mechanisms and biomedical applications. Int Immunopharmacol. 2011; 11(7):833–41. [PubMed: 21296197]
8. Babensee JE. Interaction of dendritic cells with biomaterials. Semin Immunol. 2008; 20(2):101–8. [PubMed: 18054498]
9. Fotin-Mleczek M, Duchardt KM, Lorenz C, Pfeiffer R, Ojkić-Zrna S, Probst J, et al. Messenger RNA-based vaccines with dual activity induce balanced TLR-7 dependent adaptive immune responses and provide antitumor activity. J Immunother. 2011; 34(1):1–15. [PubMed: 21150709]
10. Chen WC, Kawasaki N, Nycholat CM, Han S, Pilotte J, Crocker PR, et al. Antigen delivery to macrophages using liposomal nanoparticles targeting sialoadhesin/CD169. PLoS ONE. 2012; 7(6):e39039. [PubMed: 22723922]

11. Zhang T, Wang C-Y, Zhang W, Gao Y-W, Yang S-T, Wang T-C, et al. Generation and characterization of a fusion protein of single-chain fragment variable antibody against hemagglutinin antigen of avian influenza virus and truncated protamine. Vaccine. 2010; 28(23): 3949–55. [PubMed: 20382243]
12. Martínez Gómez JM, Fischer S, Csaba N, Kündig TM, Merkle HP, Gander B, et al. A protective allergy vaccine based on CpG- and protamine-containing PLGA microparticles. Pharm Res. 2007; 24(10):1927–35. [PubMed: 17541735]
13. Okada H. Brain tumor immunotherapy with type-1 polarizing strategies. Ann N Y Acad Sci. 2009; 1174:18–23. [PubMed: 19769732]
14. Jun YJ, Kim JH, Choi SJ, Lee HJ, Jun MJ, Sohn YS. A tetra(L-lysine)-grafted poly(organophosphazene) for gene delivery. Bioorg Med Chem Lett. 2007; 17(11):2975–8. [PubMed: 17428658]
15. Maubant S, Banissi C, Beck S, Chauvat A, Carpentier AF. Adjuvant properties of Cytosine-phosphate-guanosine oligodeoxynucleotide in combination with various polycations in an ovalbumin-vaccine model. Nucleic Acid Ther. 2011; 21(4):231–40. [PubMed: 21787231]
16. Midoux P, Breuzard G, Gomez JP, Pichon C. Polymer-based gene delivery: a current review on the uptake and intracellular trafficking of polyplexes. Curr Gene Ther. 2008; 8(5):335–52. [PubMed: 18855631]
17. Yeeprae W, Kawakami S, Yamashita F, Hashida M. Effect of mannose density on mannose receptor-mediated cellular uptake of mannosylated O/W emulsions by macrophages. J Controlled Release. 2006; 114(2):193–201.
18. Faraasen S, Vörös J, Csúcs G, Textor M, Merkle HP, Walter E. Ligand-specific targeting of microspheres to phagocytes by surface modification with poly(L-lysine)-grafted poly(ethylene glycol) conjugate. Pharm Res. 2003; 20(2):237–46. [PubMed: 12636162]
19. White KL, Rades T, Furneaux RH, Tyler PC, Hook S. Mannosylated liposomes as antigen delivery vehicles for targeting to dendritic cells. J Pharm Pharmacol. 2006; 58(6):729–37. [PubMed: 16734974]
20. Wattendorf U, Coullerez G, Vörös J, Textor M, Merkle HP. Mannose-based molecular patterns on stealth microspheres for receptor-specific targeting of human antigen-presenting cells. Langmuir. 2008; 24(20):11790–802. [PubMed: 18785716]
21. Song X, Xia B, Stowell SR, Lasanajak Y, Smith DF, Cummings RD. Novel fluorescent glycan microarray strategy reveals ligands for galectins. Chem Biol. 2009; 16(1):36–47. [PubMed: 19171304]
22. Disney MD, Seeberger PH. The use of carbohydrate microarrays to study carbohydrate-cell interactions and to detect pathogens. Chem Biol. 2004; 11(12):1701–7. [PubMed: 15610854]
23. Ratner DM, Adams EW, Su J, O'Keefe BR, Mrksich M, Seeberger PH. Probing protein-carbohydrate interactions with microarrays of synthetic oligosaccharides. Chem BioChem. 2004; 5(3):379–83.
24. Disney MD, Seeberger PH. The use of carbohydrate microarrays to study carbohydrate-cell interactions and to detect pathogens. Chem Biol. 2004; 11(12):1701–7. [PubMed: 15610854]
25. Taylor ME, Drickamer K. Structural insights into what glycan arrays tell us about how glycan-binding proteins interact with their ligands. Glycobiology. 2009; 19(11):1155–62. [PubMed: 19528664]
26. Van Vliet SJ, van Liempt E, Saeland E, Aarnoudse CA, Appelmelk B, Irimura T, et al. Carbohydrate profiling reveals a distinctive role for the C-type lectin MGL in the recognition of helminth parasites and tumor antigens by dendritic cells. Int Immunol. 2005; 17(5):661–9. [PubMed: 15802303]
27. van Vliet SJ, van Liempt E, Saeland E, Aarnoudse CA, Appelmelk B, Irimura T, et al. Carbohydrate profiling reveals a distinctive role for the C-type lectin MGL in the recognition of helminth parasites and tumor antigens by dendritic cells. Int Immunol. 2005; 17(5):661–9. [PubMed: 15802303]
28. Guo Y, Feinberg H, Conroy E, Mitchell DA, Alvarez R, Blixt O, et al. Structural basis for distinct ligand-binding and targeting properties of the receptors DC-SIGN and DC-SIGNR. Nat Struct Mol Biol. 2004; 11(7):591–8. [PubMed: 15195147]

29. Feinberg H, Castelli R, Drickamer K, Seeberger PH, Weis WI. Multiple modes of binding enhance the affinity of DC-SIGN for high mannose N-Linked glycans found on viral glycoproteins. J Bio Chem. 2007; 282(6):4202–4209. [PubMed: 17150970]
30. Song X, Lasanajak Y, Rivera-Marrero C, Luyai A, Willard M, Smith DF, et al. Generation of a natural glycan microarray using 9-fluorenylmethyl chloroformate (FmocCl) as a cleavable fluorescent tag. Anal Biochem. 2009; 395(2):151–60. [PubMed: 19699706]
31. Song X, Lasanajak Y, Xia B, Smith DF, Cummings RD. Fluorescent glycosylamides produced by microscale derivatization of free glycans for natural glycan microarrays. ACS Chem Bio. 2009; 4(9):741–50. [PubMed: 19618966]
32. Song E-H, Pohl NL. Carbohydrate arrays: recent developments in fabrication and detection methods with applications. Curr Opin Chem Biol. 2009; 13(5–6):626–32. [PubMed: 19853494]
33. Jaipuri FA, Pohl NL. Toward solution-phase automated iterative synthesis: fluorous-tag assisted solution-phase synthesis of linear and branched mannose oligomers. Org Biomol Chem. 2008; 6(15):2686–91. [PubMed: 18633525]
34. Fukuda, M. Current Protocols in Molecular Biology [Internet]. John Wiley & Sons, Inc; 2001. Chemical labeling of carbohydrates by oxidation and sodium borohydride reduction. [cited 2013 Jun 16]. Available from: http://onlinelibrary.wiley.com/doi/10.1002/0471142727.mb1705s26/abstract
35. Yoshida M, Babensee JE. Molecular aspects of microparticle phagocytosis by dendritic cells. J Biomater Sci Polym Ed. 2006; 17(8):893–907. [PubMed: 17024879]
36. Kou PM, Babensee JE. Validation of a high-throughput methodology to assess the effects of biomaterials on dendritic cell phenotype. Acta Biomater. 2010; 6(7):2621–30. [PubMed: 20097314]
37. Manavalan JS, Rossi PC, Vlad G, Piazza F, Yarilina A, Cortesini R, et al. High expression of ILT3 and ILT4 is a general feature of tolerogenic dendritic cells. Transpl Immunol. 2003; 11(3–4):245–58. [PubMed: 12967778]
38. MacCoubrey I, Moore P, Haugland R. Quantitative fluorescence measurements of cell viability (cytotoxicity) with a multi-well plate scanner. J Cell Biol. 1990; 5 pt 2(111):58a.
39. Oyelaran O, Li Q, Farnsworth D, Gildersleeve JC. Microarrays with varying carbohydrate density reveal distinct subpopulations of serum antibodies. J Proteome Res. 2009; 8(7):3529–38. [PubMed: 19366269]
40. Holla A, Skerra A. Comparative analysis reveals selective recognition of glycans by the dendritic cell receptors DC-SIGN and Langerin. Protein Eng Des Sel. 2011; 24(9):659–669. [PubMed: 21540232]
41. Oyelaran O, Li Q, Farnsworth D, Gildersleeve JC. Microarrays with varying carbohydrate density reveal distinct subpopulations of serum antibodies. J Proteome Res. 2009; 8(7):3529–38. [PubMed: 19366269]
42. Tao S-C, Li Y, Zhou J, Qian J, Schnaar RL, Zhang Y, et al. Lectin microarrays identify cell-specific and functionally significant cell surface glycan markers. Glycobiology. 2008; 18(10):761–9. [PubMed: 18625848]
43. Blixt O, Han S, Liao L, Zeng Y, Hoffmann J, Futakawa S, et al. Sialoside analogue arrays for rapid identification of high affinity siglec ligands. J Am Chem Soc. 2008; 130(21):6680–1. [PubMed: 18452295]
44. Ajit Varki, RDC. Essentials of Glycobiology [Internet]. 2009. [cited 2013 Jun 29]. Available from: http://www.ncbi.nlm.nih.gov.www.library.gatech.edu:2048/books/NBK1908/
45. Ribeiro S, de Araujo Soares RM, Sales Alviano C, Da Silva EF, De Souza W, Angluster J. Cell-surface carbohydrates of Entamoeba invadens. Parasitol Res. 1997; 83(8):801–5. [PubMed: 9342747]
46. Chapman A, Trowbridge IS, Hyman R, Kornfeld S. Structure of the lipid-linked oligosaccharides that accumulate in class E Thy-1-negative mutant lymphomas. Cell. 1979; 17(3):509–15. [PubMed: 476829]
47. Chapman A, Fujimoto K, Kornfeld S. The primary glycosylation defect in class E Thy-1-negative mutant mouse lymphoma cells is an inability to synthesize dolichol-P-mannose. J Biol Chem. 1980; 255(10):4441–6. [PubMed: 7372584]

48. Trowbridge IS, Hyman R. Abnormal lipid-linked oligosaccharides in class E thy-1-negative mutant lymphomas. Cell. 1979; 17(3):503–8. [PubMed: 476828]
49. Adams EW, Ratner DM, Seeberger PH, Hacohen N. Carbohydrate-mediated targeting of antigen to dendritic cells leads to enhanced presentation of antigen to T cells. Chem BioChem. 2008; 9(2): 294–303.
50. Johnson TR, McLellan JS, Graham BS. Respiratory syncytial virus Glycoprotein G interacts with DC-SIGN and L-SIGN to activate ERK1 and ERK2. J Virol. 2012; 86(3):1339–47. [PubMed: 22090124]
51. Geijtenbeek TBH, Gringhuis SI. Signalling through C-type lectin receptors: shaping immune responses. Nat Rev Immunol. 2009; 9(7):465–79. [PubMed: 19521399]
52. Figdor CG, van Kooyk Y, Adema GJ. C-type lectin receptors on dendritic cells and Langerhans cells. Nat Rev Immunol. 2002; 2(2):77–84. [PubMed: 11910898]
53. Jiang H-L, Kang ML, Quan J-S, Kang SG, Akaike T, Yoo HS, et al. The potential of mannosylated chitosan microspheres to target macrophage mannose receptors in an adjuvant-delivery system for intranasal immunization. Biomaterials. 2008; 29(12):1931–9. [PubMed: 18221992]
54. Kou PM, Pallassana N, Bowden R, Cunningham B, Joy A, Kohn J, et al. Predicting biomaterial property-dendritic cell phenotype relationships from the multivariate analysis of responses to polymethacrylates. Biomaterials. 2012; 33(6):1699–713. [PubMed: 22136715]
55. Kou PM, Schwartz Z, Boyan BD, Babensee JE. Dendritic cell responses to surface properties of clinical titanium surfaces. Acta Biomater. 2011; 7(3):1354–63. [PubMed: 20977948]
56. Hsu S-C, Tsai T-H, Kawasaki H, Chen C-H, Plunkett B, Lee RT, et al. Antigen coupled with Lewis-x trisaccharides elicits potent immune responses in mice. J Allergy Clin Immunol. 2007; 119(6):1522–8. [PubMed: 17353042]
57. Trombetta ES, Ebersold M, Garrett W, Pypaert M, Mellman I. Activation of lysosomal function during dendritic cell maturation. Science. 2003; 299(5611):1400–3. [PubMed: 12610307]
58. Kikuchi K, Yanagawa Y, Onoé K. CCR7 ligand-enhanced phagocytosis of various antigens in mature dendritic cells-time course and antigen distribution different from phagocytosis in immature dendritic cells. Microbiol Immunol. 2005; 49(6):535–44. [PubMed: 15965301]
59. Hsu S-C, Chen C-H, Tsai S-H, Kawasaki H, Hung C-H, Chu Y-T, et al. Functional interaction of common allergens and a C-type lectin receptor, dendritic cell-specific ICAM3-grabbing non-integrin (DC-SIGN), on human dendritic cells. J Biol Chem. 2010; 285(11):7903–10. [PubMed: 20080962]
60. Bonifaz L, Bonnyay D, Mahnke K, Rivera M, Nussenzweig MC, Steinman RM. Efficient targeting of protein antigen to the dendritic cell receptor DEC-205 in the steady state leads to antigen presentation on major histocompatibility complex class I products and peripheral CD8+ T cell tolerance. The Journal of Experimental Medicine. 2002; 196(12):1627–1638. [PubMed: 12486105]
61. Roy R, Baek M-G. Glycodendrimers: novel glycotope isosteres unmasking sugar coding. Case study with T-antigen markers from breast cancer MUC1 glycoprotein. Reviews in Molecular Biotechnology. 2002; 90(3–4):291–309. [PubMed: 12071230]
62. Savage P, Millrain M, Dimakou S, Stebbing J, Dyson J. Expansion of CD8+ cytotoxic T cells in vitro and in vivo using MHC class I tetramers. Tumour Biol. 2007; 28(2):70–6. [PubMed: 17264539]
63. Muckerheide A, Apple RJ, Pesce AJ, Michael JG. Cationization of protein antigens. I. Alteration of immunogenic properties. J Immunol. 1987; 138(3):833–7. [PubMed: 2433331]

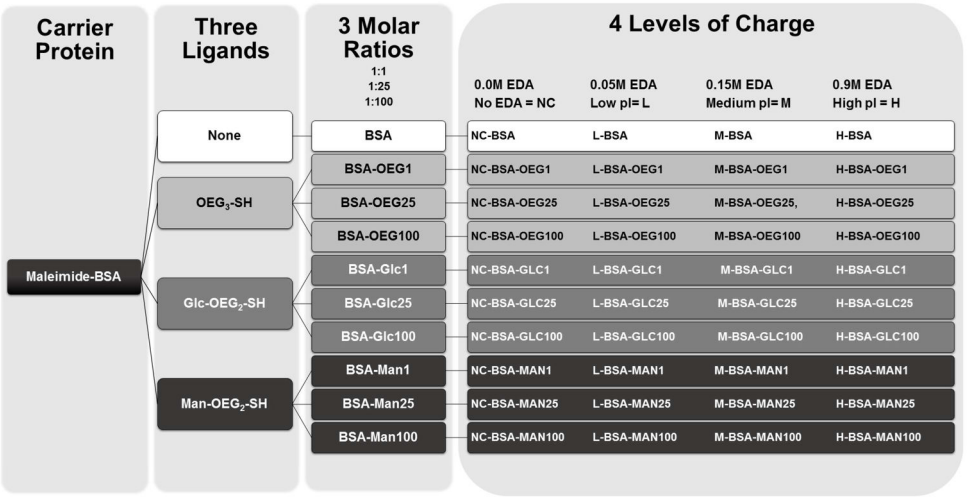

Figure 1.

Process and characterization methodology that was used to create the 40 conjugates tested in Figure 4.

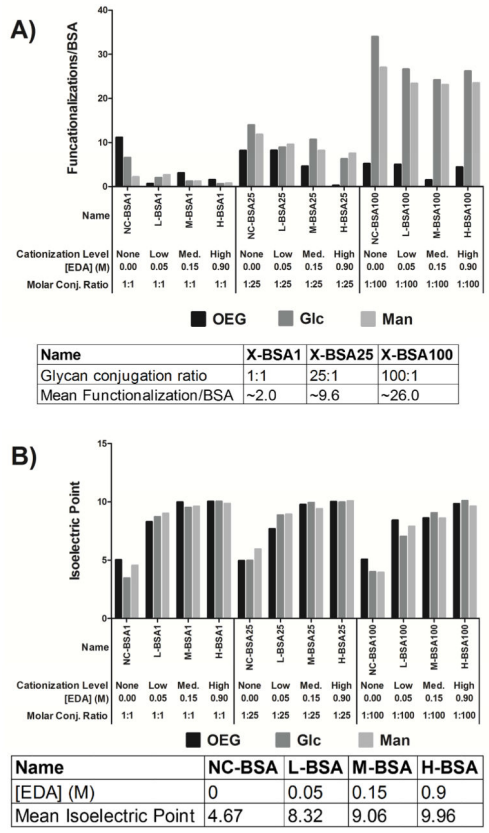

Name	X-BSA1	X-BSA25	X-BSA100
Glycan conjugation ratio	1:1	25:1	100:1
Mean Functionalization/BSA	~2.0	~9.6	~26.0

Name	NC-BSA	L-BSA	M-BSA	H-BSA
[EDA] (M)	0	0.05	0.15	0.9
Mean Isoelectric Point	4.67	8.32	9.06	9.96

Figure 2.

Mass and isoelectric point of all conjugates. All conjugates from Figure 1 were characterized for their mass and average number of ligands per BSA (A) and for their mean isoelectric point (B). The average mass of each conjugate discussed in Figure 1 was determined via MALDI mass spectrometry. The arithmetic mean of the mass peak profile was calculated and plotted in (A). The table under (A) shows the average number of ligands per BSA across each level of cationization. The isoelectric point was calculated for each conjugate from the conjugate's ζ-potential versus pH plot and can be seen in (B). The average isoelectric point at each ligand density can also be seen in the table below (B).

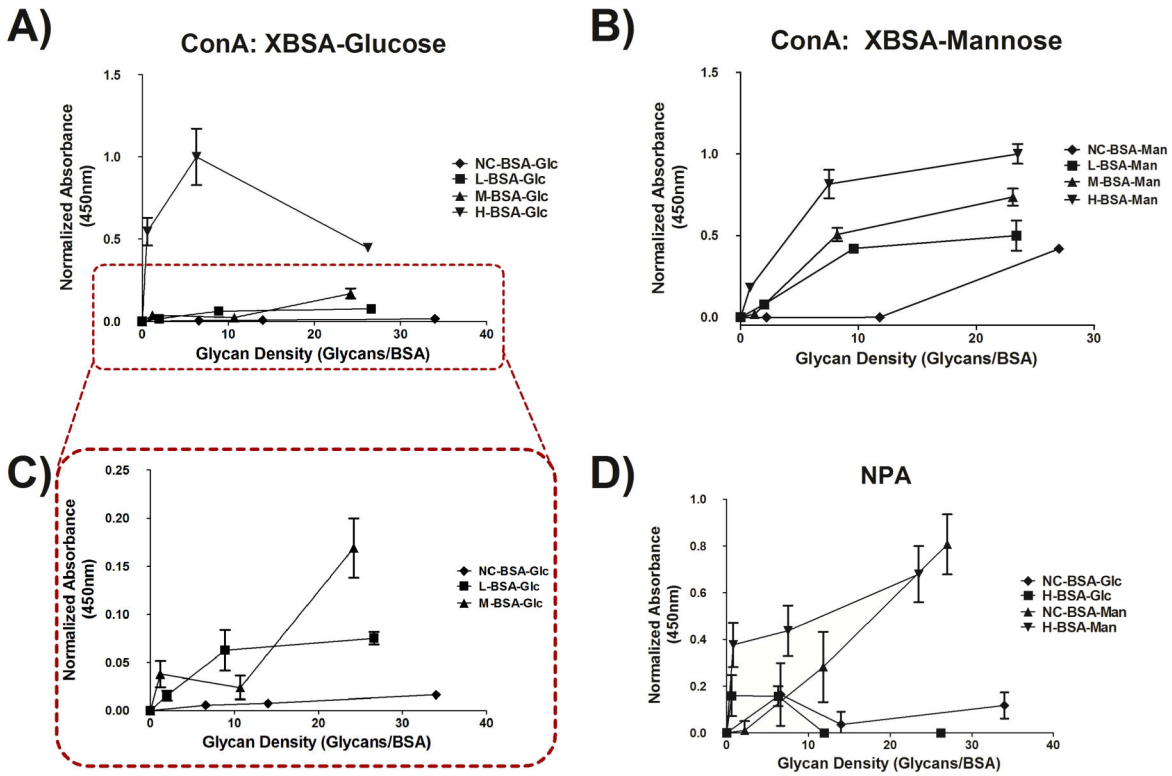

Figure 3.

ELLA using plant lectins on the adsorbed glycoconjugates from Figure 1 in a 384 well plate. Binding of the lectin ConA to adsorbed glucose glycoconjugates (A) and to adsorbed mannose glycoconjugates (B) can be seen. The subset of (A) shows a consistent trend with what would be expected. Also, sugar linkage to carriers shows lectin binding specificity as shown by (D) which shows that NPA (mannose specific) binds to the mannose glycoconjugates with a much high affinity than it does to glucose glycoconjugates. n=3 for A and B, n=5 for D. Error bars represent SE. Conjugate absorbance normalized by treatment with highest absorbance.

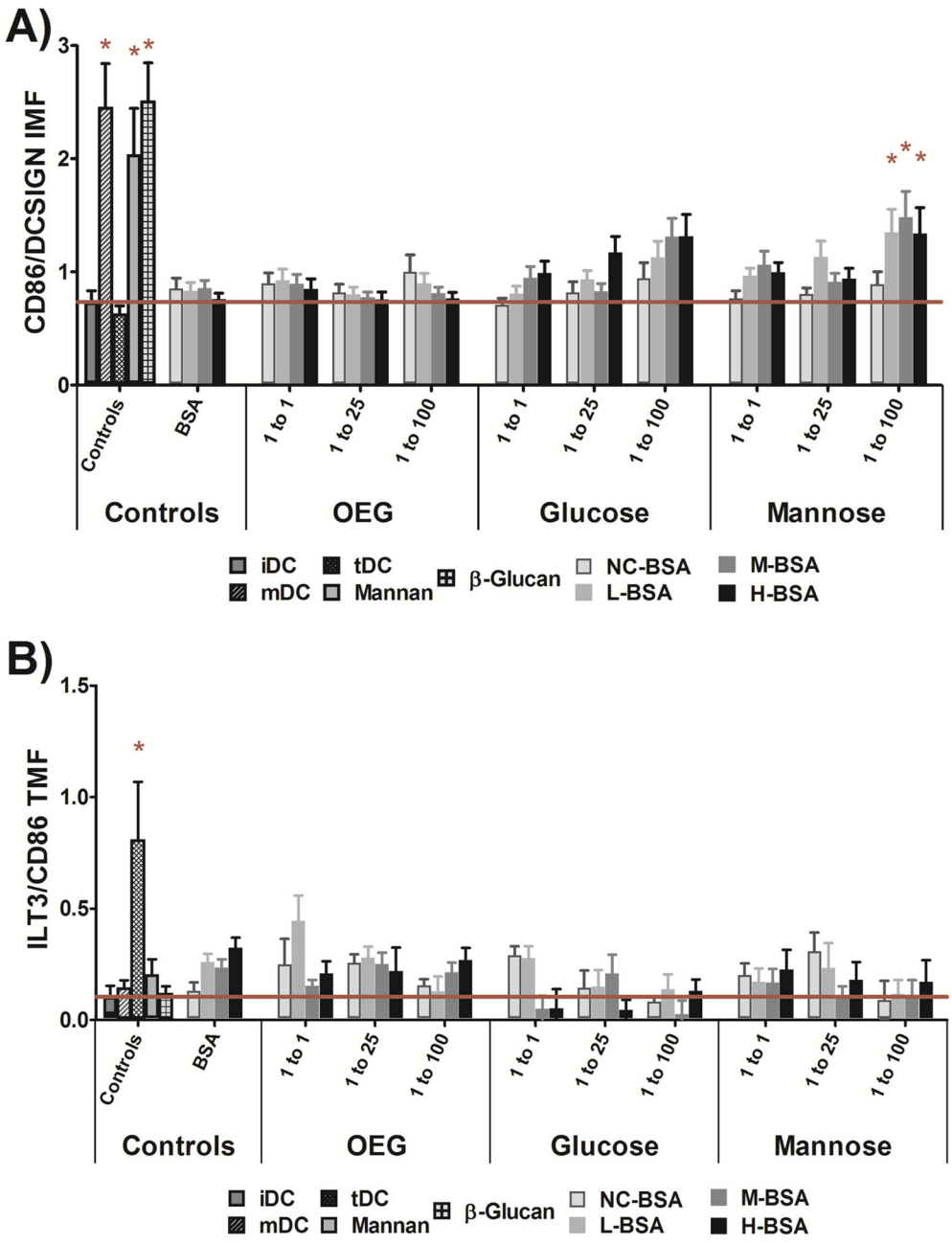

Figure 4.

Dendritic cell IMF and TMF levels in response to glycoconjugate adsorbed well surfaces. All positive controls were statistically different from iDC and L-, M-, and H-BSAMan100 conjugates showed a statistically increased fold change in IMF (A). No treatment showed a statistically increased TMF level as compared to iDCs (B). The positive control, tDC, did show an increased level of TMF as compared to iDC (B). Error Bars Represent ±SE, * = P<0.05 from iDC, n=13 donors, red line indicates mean iDC response.

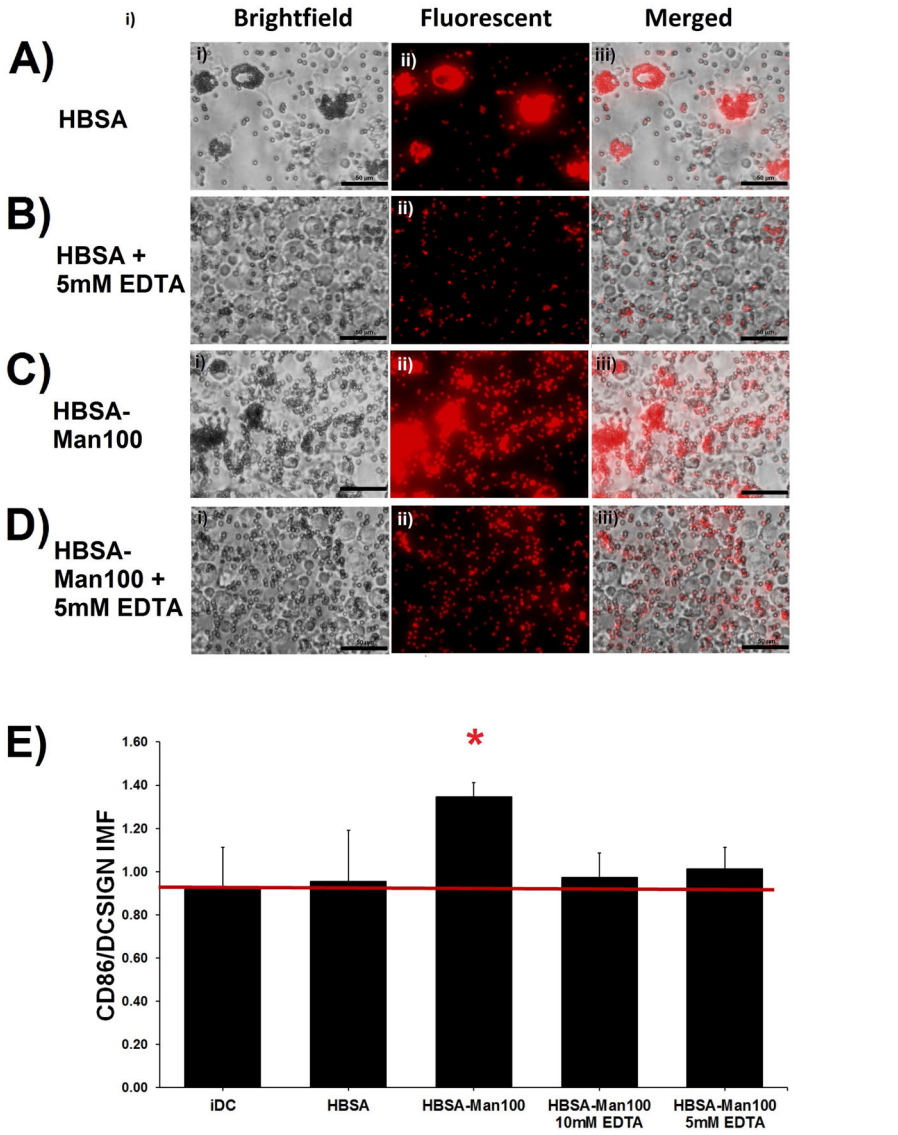

Figure 5.

DC response to H-BSA-Man100 conjugates adsorbed onto 1.0μm fluorescent polystyrene beads and subsequent IMF in the presence of 10mM or 5mM EDTA. DCs phagocytized H-BSA and H-BSA-Man100 coated beads to a much greater extent than they did H-BSA-Man100 coated beads in the presence of 5mM EDTA (A–D). No fold change in IMF was seen between iDCs and the EDTA treated cells. The unblocked HBSA-Man100 conjugate showed a statistical increase in IMF (D). n=4 donors. Error bars represent standard error, red line indicates mean iDC response, * indicates statistical difference from iDC.

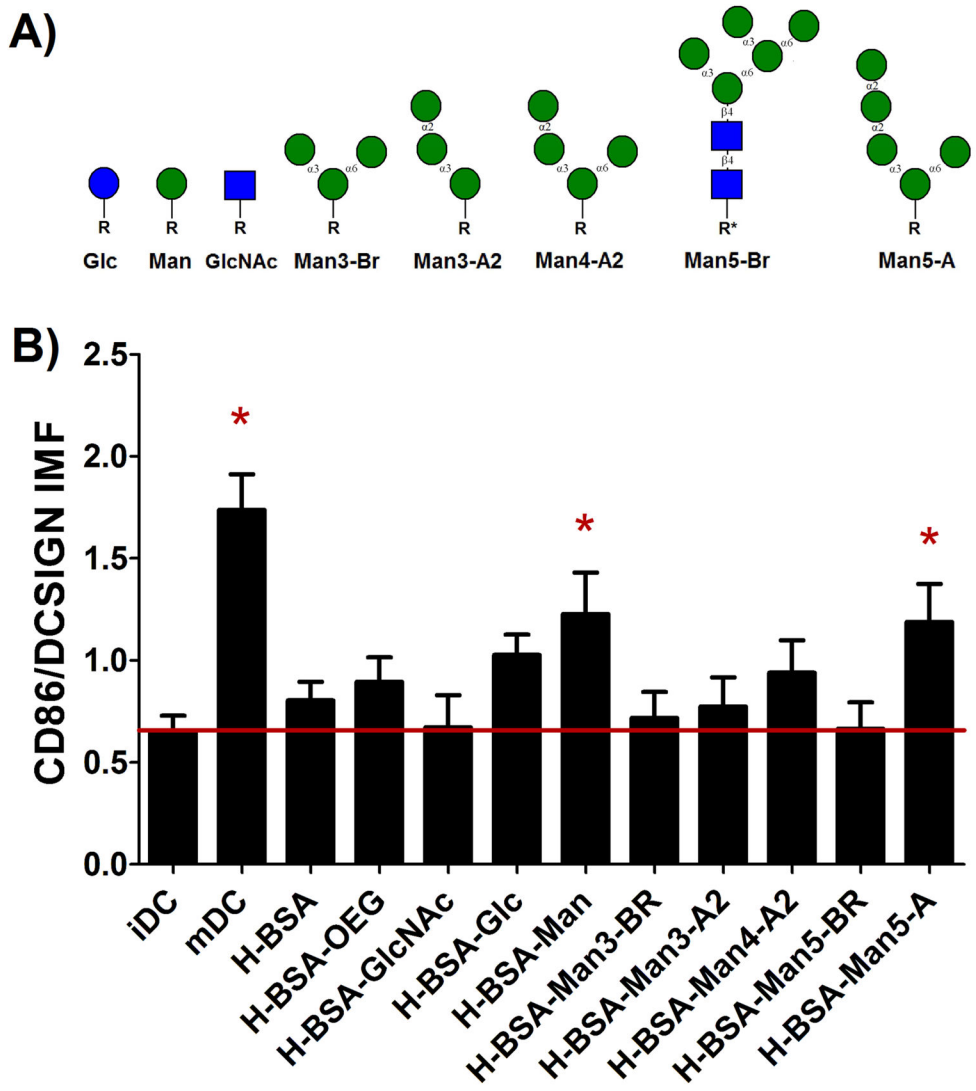

Figure 6.

Assessment of DC phenotype in response to poly-mannose structures. The structures tested can be seen in (A). Here R and R* represent the linker used for the glycan. R= $(CH_2CH_2O)_3SH$ and R*= AEAB-$NH_2C(CH_2)_3SH$, The IMF was assessed for all adsorbed conjugates and H-BSA-Man and H-BSA-Man5-A had had a statistically increased expression over iDC (B). mDCs also showed a statistical increase in IMF. n=17 donors. Error bars represent standard error, red line indicates mean iDC response, * indicates statistical difference from iDC.

Table 1

IMF parameter estimates for the model seen in equation 1a using categorical isoelectric point and density.

Variable	βs	β Parameter Estimate	Standard Error	t Value	Pr > |t|
Intercept	β_1	0.923	0.016	59.57	<.0001
Isoelectric High	β_2	0.172	0.034	5.12	<.0001
Isoelectric Med.	β_3	0.157	0.032	4.85	<.0001
Isoelectric Low.	β_4	−0.008	0.049	−0.16	0.8718
Ligand OEG	β_5	−0.004	0.044	−0.09	0.9245
Ligand Glc	β_6	0.015	0.048	0.3	0.7622
Ligand Man	β_7	0.065	0.047	1.41	0.1602
Density High	β_8	0.381	0.037	10.21	<.0001
Density Med.	β_9	0.097	0.031	3.12	0.0019
*Density Low***	β_{10}	0	.	.	.
*Donor**	$\beta_{11–22}$	−0.594 – 0.660	0.058	−10.21 – 11.35	<.0001

* All donor estimates, standard errors, t values, and probabilities can be seen in the Error! Reference source not found. in the supplemental.

** Low density conjugates varied linearly with the control due to no difference between cell response to low density and no ligand groups. Thus, this group had to be removed from the model.

Table 2

TMF parameter estimates for equation 1B using categorical isoelectric point and density.

Variable	βs	β Parameter Estimate	Standard Error	t Value	Pr > |t|
Intercept	β_1	0.120	0.005	22.15	<.0001
Isoelectric High	β_2	−0.024	0.012	−2.06	0.0397
Isoelectric Med.	β_3	−0.0002	0.011	−0.02	0.9854
Isoelectric Low	β_4	0.035	0.017	2.09	0.0372
Ligand OEG	β_5	0.007	0.015	0.43	0.6681
Ligand Glc	β_6	−0.029	0.017	−1.74	0.0819
Ligand Man	β_7	−0.025	0.016	−1.54	0.1253
Density High	β_8	−0.064	0.013	−4.92	<.0001
Density Med.	β_9	−0.028	0.011	−2.55	0.0111
*Density Low***	β_{10}	0	.	.	.
*Donor**	$\beta_{11–22}$	−0.594 – 0.660	0.058	−6.22 – 10.57	<.0001

* All donor estimates, standard errors, t values, and probabilities can be seen in the Table S2 in the supplemental.

** Low density conjugates varied linearly with the control due to no difference between cell response to low density and no ligand groups. Thus, this group had to be removed from the model.

Table 3

IMF parameter estimates for model 2 using categorical isoelectric point and density.

Variable	βs	β Parameter Estimate	Std. Error	t Value	Pr > |t|
Intercept	β1	1.013	0.047	21.52	<.0001
Density High	β2	0.091	0.129	0.70	0.4852
Density Med	β3	−0.053	0.168	−0.32	0.7518
Density Low	β4	−0.171	0.213	−0.80	0.4232
*OEG***	β5	0	.	.	.
Glc	β6	0.420	0.141	3.68	0.0004
GlcNac	β7	0.135	0.229	0.59	0.5561
Man	β8	0.476	0.212	2.24	0.0270
Alpha	β9	0.488	0.212	2.06	0.0416
Branch	β10	0.129	0.154	0.83	0.4065
*Donors 1–16**	β11–26	−0.451 – 1.075	0.227	−1.98 – 4.23	0.0005

* All donor estimates, standard errors, t values, and probabilities can be seen in the Table S3 in the supplemental.

** OEG conjugates varied linearly with the control due to no difference between cell response to OEG and no ligand groups. Thus, this group had to be removed from the model.